electronics

MDPI

Article

Advanced Steering Stability Controls for Autonomous Articulated Vehicles Based on Differential Braking

Jesus Felez

Mechanical Engineering Department, Universidad Politécnica de Madrid, 28006 Madrid, Spain; jesus.felez@upm.es

Abstract

Articulated vehicles are essential for global freight transportation but are highly susceptible to instability phenomena such as jackknifing, trailer sway, and rollover, particularly under high-speed or emergency maneuvers. These challenges become even more critical in the context of autonomous driving, where stability must be guaranteed without human intervention. Conventional systems like Electronic Stability Control (ESC) and Roll Stability Control (RSC) provide reactive interventions but lack predictive capability, while other advanced methods often address isolated objectives. To overcome these limitations, this paper proposes a Model Predictive Control (MPC)-based control strategy that integrates trajectory tracking, yaw stability, and longitudinal speed regulation within a unified optimization framework, using differential braking as the primary actuator. A dynamic model of a tractor–semitrailer combination was developed, and the proposed controller was validated through high-fidelity simulations under varying operating conditions, including speeds exceeding the critical threshold of 31.04 m/s. Results demonstrate that the MPC-based system effectively mitigates instability, reduces articulation angle and yaw rate deviations, and maintains accurate path tracking while proactively managing vehicle speed. These findings highlight MPC's potential as a cornerstone technology for safe and reliable autonomous operation of articulated vehicles. Future work will focus on experimental validation and multi-actuator coordination to further enhance performance.

Keywords: autonomous articulated vehicles; Model Predictive Control (MPC); differential braking; yaw stability; trajectory tracking; longitudinal speed regulation; vehicle dynamics; stability control

Check for updates

Academic Editor: Cecilio Angulo

Received: 20 December 2025
Revised: 22 January 2026
Accepted: 28 January 2026
Published: 30 January 2026

Copyright: © 2026 by the author. Licensee MDPI, Basel, Switzerland. This article is an open access article distributed under the terms and conditions of the Creative Commons Attribution (CC BY) license.

1. Introduction

Road freight transportation remains the dominant mode for goods distribution worldwide, with articulated vehicles playing a critical role in this sector due to their flexibility and cost-effectiveness. However, these vehicles exhibit complex dynamic behavior that introduces significant safety challenges. Articulated configurations—such as tractor–semitrailers and multi-trailer combinations—are particularly vulnerable to instability phenomena including jackknifing, trailer sway (snaking), and rollover. These events typically occur under high-speed conditions, abrupt steering maneuvers, or uneven load distributions, and they not only compromise vehicle control but also increase accident severity compared to single-unit vehicles [1,2].

In general, the following types of instability may occur [3].

The first type is divergent instability, which occurs when the mass of the trailer is partially supported by the towing vehicle at the coupling point. If the vertical force exerted

by the trailer on the towing vehicle becomes excessively large, the vehicle combination exhibits a monotonically unstable motion, ultimately compromising overall stability.

The second type is unstable oscillatory yaw motion. In this case, the oscillation amplitude is unbounded, even under non-linear conditions. As the amplitude increases, the slip angle also grows, which reduces the average cornering stiffness due to the digressive, non-linear tire cornering force characteristic. This progressive reduction in cornering stiffness exacerbates the instability, making the situation increasingly critical.

In this case, two distinct types of trailer oscillations can be identified [4], as illustrated in Figure 1.

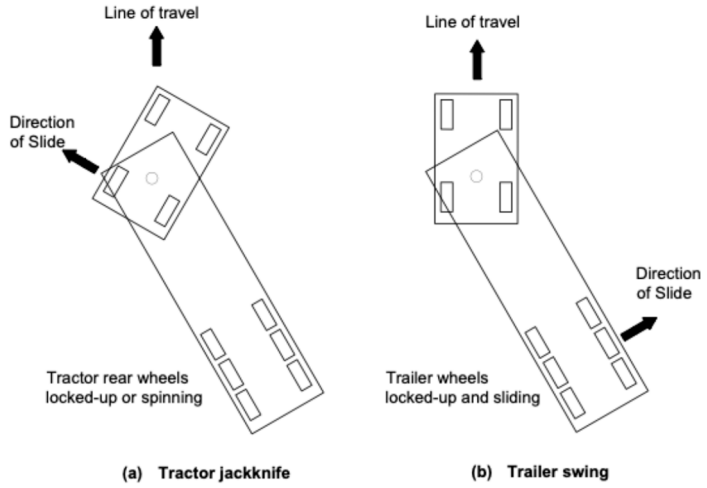

Figure 1. Two jack-knife possibilities of a tractor-semitrailer.

The tractor may jackknife (Figure 1a) either under power or during braking, particularly when the rear wheels of the tractor lose grip or traction. This condition results in an acute angle between the tractor and trailer, severely compromising maneuverability and safety.

Trailer swing (Figure 1b) may occur when the trailer axle wheels lock during braking, causing the rear of the trailer to swing outward and increasing the risk of collision. Trailer swing is often considered a form of yaw instability, even though the vehicle combination may remain mathematically stable.

A complete analysis of articulated vehicles can be found in [5].

The progression from passive mechanical systems to active and intelligent controllers reflects the growing complexity of articulated vehicle dynamics and the demand for autonomous driving capabilities. Traditional systems such as Electronic Stability Control (ESC) and Roll Stability Control (RSC) provide reactive interventions but lack predictive capabilities, limiting their effectiveness under extreme conditions [1] and are insufficient for the demands of autonomous operation.

Another significant research challenge in the automotive industry is the development of autonomous vehicles, which are defined as vehicles capable of perceiving their surroundings and replicating human driving and control abilities [6]. The degree of autonomy in a vehicle is categorized into six levels. Currently, several companies are focusing on the development of Level 4 and Level 5 vehicles [7], although the highest level available on the market today is Tesla's Autopilot, classified as Level 3. The transition toward autonomous heavy-duty vehicles further amplifies the need for advanced stability control strategies capable of managing nonlinear dynamics, multi-body interactions, and stringent safety constraints without human intervention.

The growing demand for autonomous driving technologies in heavy-duty vehicles further emphasizes the need for robust stability control systems. Autonomous articulated trucks must execute complex maneuvers without human intervention, requiring advanced control strategies that can manage nonlinear dynamics, multi-body interactions, and stringent safety constraints. Recent research has explored various advanced control approaches, including Fuzzy Logic Control (FLC), Sliding Mode Control (SMC), and Model Predictive Control (MPC). FLC and SMC offer robustness against parameter variations and disturbances but are limited in predictive capability and multi-variable constraint handling. MPC, on the other hand, provides a predictive framework that optimizes control actions over a receding horizon while systematically managing constraints, making it particularly suitable for complex articulated vehicle dynamics. Despite these advantages, most existing studies focus on isolated objectives such as yaw stability or trajectory tracking, leaving a gap in holistic solutions for autonomous articulated vehicles.

With respect to the control system, the MPC is an advanced control method [8]. This technique has been successfully used in many industrial applications, like thermal energy control [9], collision avoidance [10], vehicle stability [11], and energy management [12]. The MPC capacity of working with non-linear systems makes it appropriate for several applications in engineering, being of particular interest its use in autonomous vehicles [13].

Several automotive companies, such as Ford, BMW, Honda, PSA, and Toyota, are actively investigating the implementation of advanced control systems. These systems have a wide range of applications, including traction control, semi-active suspension control, vehicle stability management, and energy optimization in electric vehicles. Although such control strategies typically involve high computational demands, the integration of multi-parametric programming with an appropriately designed prediction horizon can significantly reduce the computational burden on vehicle microcontrollers, enabling real-time execution in on-board systems.

1.1. State of the Art

The stability of articulated vehicles under high-speed conditions and emergency maneuvers has been extensively studied, leading to the development of several advanced control strategies. These approaches differ in their mathematical foundations, robustness to uncertainties, and computational requirements.

Among them, MPC has emerged as the dominant methodology. MPC predicts future system states over a receding horizon and computes optimal control actions by solving a constrained optimization problem at each time step. Its ability to handle multi-variable systems and incorporate operational constraints makes it particularly suitable for articulated vehicles with complex dynamics. Studies such as [14–16] demonstrate the effectiveness of MPC in trajectory tracking and yaw stability control. However, its main limitation lies in the high computational demand, which requires efficient algorithms for real-time implementation.

Recent studies provide compelling evidence of the effectiveness of MPC in improving articulated vehicle stability and maneuverability. Reference [15] demonstrated that MPC with differential braking achieved a maximum articulation angle reduction of 1.6° while maintaining precise path tracking under dynamic conditions.

The comparative authority of differential braking has also been validated experimentally. Reference [14] conclusively demonstrated that “differential braking has much more capacity when it is applied to the tractor” compared to trailer-only application. This observation emphasizes the critical role of tractor braking torque in generating corrective yaw moments and maintaining overall vehicle stability during emergency maneuvers.

Finally, preventive control strategies have shown remarkable potential in enhancing vehicle performance under challenging conditions. Reference [17] reported that pre-emptive Nonlinear MPC achieved up to a 34% increase in maximum entry speeds under high-friction conditions and up to 60% under low-friction conditions. These improvements demonstrate the value of predictive algorithms in anticipating instability and optimizing control actions before critical thresholds are reached.

In addition to physical testing, high-fidelity simulation platforms remain the predominant tool for controller development and preliminary validation. Most studies [14,15,17,18] employ MATLAB/Simulink (R2025b, https://mathworks.com) environments integrated with CarSim (https://www.carsim.com/products/carsim/index.php, accessed on 27 January 2026) to model complex vehicle dynamics accurately. Another widely explored approach is Fuzzy Logic Control, including fuzzy PID variants. Fuzzy Logic Control (FLC) and its derivative, fuzzy PID control, have been widely investigated for improving the lateral stability of articulated vehicles due to their robustness against parameter variations and adaptability to nonlinear dynamics. These controllers rely on linguistic rules and membership functions rather than precise mathematical models, making them robust to parameter variations and load changes. Refs. [19,20] highlight the intuitive design and adaptability of fuzzy controllers in managing nonlinearities.

Recent studies have demonstrated the effectiveness of fuzzy PID controllers in enhancing yaw stability and articulation control. Reference [21] reported that a multi-objective fuzzy PID control strategy achieved a 45.45% reduction in the tractor's maximum yaw rate and a 4.55% reduction in the semi-trailer's yaw rate during dynamic maneuvers. Furthermore, the same study showed a 46.67% decrease in maximum articulation angle, significantly improving coupling stability. In terms of lateral tracking, Li et al. observed a 3.71% reduction in tractor lateral displacement deviation and a 5.45% reduction for the semi-trailer, confirming the controller's ability to maintain accurate trajectory tracking under challenging conditions.

Complementary findings were presented by [19], who demonstrated remarkable improvements in sideslip control. Their fuzzy logic-based approach reduced the tractor's sideslip angle from 92.83° to a range of 8.67–10.92°, while the semi-trailer's sideslip angle decreased from 61.02° to 25.66–39.79°. These results highlight the capacity of fuzzy controllers to mitigate severe lateral instability phenomena such as snaking and jackknifing.

Fuzzy PID controllers are favored for their robustness to parameter variations, which are common in articulated vehicles with fluctuating payloads and road conditions. Unlike model-based approaches, fuzzy controllers do not require highly accurate system models, reducing implementation complexity. However, their performance strongly depends on the quality of the rule base and membership functions, and they may exhibit limitations in predictive capability compared to advanced optimization-based methods such as MPC.

The robustness of these control strategies has been validated under highly challenging scenarios. Reference [19] and subsequent studies evaluated performance during double lane-change maneuvers at speeds ranging from 70 to 100 km/h on low-adhesion surfaces, conditions that typically induce severe instability in articulated configurations. To ensure comprehensive analysis, these studies employed co-simulation platforms integrating TruckSim (https://www.carsim.com/products/trucksim/, accessed on 27 January 2026) with MATLAB/Simulink.

Sliding Mode Control (SMC) represents a robust nonlinear technique that forces system trajectories to follow a predefined sliding surface, ensuring invariance to matched uncertainties. References [22,23] report that SMC provides excellent robustness against disturbances and parameter variations. Despite these advantages, the chattering phenomenon

associated with SMC can lead to actuator wear and degraded performance, requiring careful design to mitigate this issue.

Sliding Mode Control (SMC) has been studied as a robust nonlinear control strategy for articulated vehicle stability due to its invariance to matched uncertainties and strong disturbance rejection capability. Unlike conventional controllers, SMC forces system trajectories to follow a predefined sliding surface, ensuring stability even under significant parameter variations and external disturbances.

Recent research by [22] introduced a phase portrait-based SMC approach that achieved a yaw damping ratio of 0.81 for both the towing vehicle and the trailer, significantly enhancing dynamic stability during high-speed maneuvers.

Earlier studies also confirm the effectiveness of SMC in multi-objective stability control. Reference [23] demonstrated that SMC provides "significant improvement in vehicle stability during transient maneuvers" and is highly effective in preventing critical instability phenomena such as rollover and jackknifing. Similarly, ref. [24] explored integrated control schemes combining active front steering and differential braking under an SMC framework, further validating its capability to maintain yaw and lateral stability in articulated configurations.

The primary advantage of SMC lies in its robustness against disturbances and invariance to matched uncertainty, making it particularly suitable for articulated vehicles operating under variable payloads and unpredictable road conditions. However, despite its strong theoretical guarantees, SMC suffers from the well-known chattering phenomenon, which can lead to actuator wear and degraded performance if not properly mitigated. This limitation necessitates careful design of smoothing strategies or higher-order sliding modes to ensure practical applicability in real-world autonomous systems.

Optimal control strategies such as the Linear Quadratic Regulator (LQR) have also been applied to articulated vehicle stability. LQR minimizes a quadratic cost function to achieve optimal performance for linearized systems. Reference [25] demonstrate its effectiveness when accurate models are available. However, its applicability is limited in nonlinear and time-varying conditions, which are common in articulated vehicle dynamics.

Adaptive Control techniques offer real-time parameter adjustment to compensate for variations in system dynamics, such as changes in payload or road conditions. References [26,27] show that adaptive controllers can maintain stability under varying operating conditions. The main drawback of these methods is the increased complexity associated with tuning multiple adaptive parameters.

Reference [27] demonstrated that "the controller can adaptively provide control actions to respond to changes in the semi-trailer's loading conditions," confirming its suitability for commercial vehicles with variable payloads. Furthermore, their study revealed that differential braking effectively reduces the fifth wheel angle during constant-speed turning maneuvers, thereby improving articulation stability. The robustness of MRAC was validated through scale model testing, using a physical tractor–semi-trailer configuration to replicate real-world dynamics. Additional experiments involved constant-speed turning maneuvers under varying load conditions, providing empirical evidence of the controller's adaptability and effectiveness in mitigating instability.

Finally, Integrated Multi-System Control strategies combine multiple actuators—such as active front steering and differential braking—to achieve coordinated control. References [16,24,28] emphasize that this approach provides superior performance in maintaining yaw and lateral stability, particularly in autonomous driving applications. However, it requires sophisticated coordination algorithms and sensor fusion to ensure seamless operation.

Reference [28] proposed a comprehensive strategy combining active steering of the tractor's front wheels, torque vectoring on the rear tractor axle, and differential braking applied to the trailer. This multi-actuator coordination enables enhanced yaw and lateral stability beyond the capabilities of single-system interventions. Similarly, ref. [24] developed an integrated control scheme that combines active front steering (AFS) with differential braking, implemented through a model reference sliding mode controller.

Table 1 summarizes the dominant control approaches identified in recent literature:

Table 1. Control Methodologies for Articulated Vehicle Stability.

Control Approach	Key Studies	Characteristics
Model Predictive Control	[14,15,17,18]	Optimization-based, predictive capability, handles constraints
Fuzzy Logic/Fuzzy PID	[19,21,29]	Robust to parameter uncertainty, intuitive rule design
Sliding Mode Control	[22,23]	Robust against disturbances, invariant to matched uncertainty
LQR/Optimal Control	[25]	Optimal performance, requires accurate model
Adaptive Control	[26,27]	Handles parameter variations, loading changes
Integrated Multi-system Control	[16,24,28]	Coordinates multiple actuators for enhanced performance

Table 2 summarizes the main metrics used to evaluate performance and its corresponding references and control method. This table shows that, if the primary objective is achieving comprehensive stability and overall performance, multi-system integration delivers the most significant improvements across multiple metrics. In contrast, MPC excels in enhancing critical speed and providing predictive control capabilities, making it particularly suitable for autonomous applications and high-speed scenarios. Meanwhile, Fuzzy Logic and Fuzzy PID controllers demonstrate effectiveness in controlling slip angle and articulation angle.

Table 2. Metrics Used to Evaluate Performance.

Metric	Key Studies	Control Method
Slip Angle Control	[19]: 88–90% tractor sideslip reduction	Fuzzy Logic/Fuzzy PID
	[28]: 84.26% trailer slip angle improvement; tractor slip angle improvement 47.86%	Integrated Multi-system Control
Yaw Rate Control	[28]: 70.20% tractor yaw rate improvement, 51.71% trailer yaw rate improvement	Integrated Multi-system Control
	[21]: 45.45% tractor yaw rate reduction	Fuzzy Logic/Fuzzy PID
Angle Control	[21]: 46.67% reduction	Fuzzy Logic/Fuzzy PID
	[19]: 52–71% reduction (from 93.32° to 27.11–44.76°)	Fuzzy Logic/Fuzzy PID
	[15]: 1.6° reduction	MPC
Critical Speed Enhancement	[17]: 60% increase (low friction), 34% increase (high friction)	MPC
Dynamic Stability	[22]: 0.81 yaw damping ratio for both units	SMC

On the other hand, several techniques are employed to prevent trailer jackknifing and trailer swing in articulated vehicle combinations.

A highly effective measure is ESC [30]. ESC systems continuously monitor vehicle dynamics and intervene by applying selective braking or reducing engine torque to maintain directional stability. These interventions are particularly valuable during sudden steering inputs or slippery road conditions, significantly reducing the likelihood of both jackknifing and trailer swing.

Anti-Lock Braking Systems (ABS) also play a critical role in stability management. ABS prevents wheel lock-up during braking [31], especially on trailer axles, ensuring tire-road contact and steering capability. This minimizes the risk of jackknifing and swing caused by locked wheels during abrupt deceleration.

Design improvements such as advanced fifth-wheel coupling systems [32] with controlled articulation or damping help reduce abrupt angular changes between tractor and trailer. These systems minimize jackknife risk during sharp turns or sudden deceleration.

In addition, active trailer sway control [33] detects oscillatory yaw motion and applies corrective braking or torque adjustments to stabilize the trailer. This technology is particularly useful for mitigating swing during high-speed lane changes or in crosswind conditions.

The choice of control parameters varies based on the instability mode being addressed. Studies targeting jackknifing prevention prioritize articulation angle control, while those addressing trailer sway focus on yaw rate deviation. Multi-objective controllers typically monitor both tractor and trailer yaw rates along with the articulation angle. These finding are summarized in Table 3.

Table 3. Control parameters based on the instability mode.

Parameter Type	Studies Using This Parameter
Yaw rate	[19,23,24,28]
Sideslip angle	[17,19,22]
Articulation/hitch angle	[14,22,23]
Fifth wheel angle	[27]
Yaw moment	[24]

Across all these techniques, differential braking emerges as a critical actuator for yaw stability. This technique involves the selective application of braking forces to individual wheels or axles, generating an asymmetric braking distribution that produces a corrective yaw moment. By counteracting undesired rotational dynamics, differential braking effectively mitigates instability phenomena such as jackknifing and trailer sway. Its implementation is cost-effective because it leverages existing braking systems, making it suitable for integration with electronic stability programs. Studies such as [1,23] confirm that tractor-only differential braking provides significant yaw control authority, although its influence on trailer dynamics is limited. Conversely, coordinated braking on both tractor and trailer units, as demonstrated by [14,15], achieves superior performance, particularly at high speeds where trailer sway becomes critical.

Several advanced control strategies have been developed to optimize the use of differential braking in articulated vehicles. Among these, MPC stands out as the dominant approach due to its predictive capabilities and systematic handling of multi-variable constraints. MPC-based controllers, such as those proposed by [14,15], integrate trajectory tracking and yaw stability objectives within a unified optimization framework. Reference [16] further extended this concept by coordinating active front steering with differ-

ential braking through a bi-level MPC structure, achieving enhanced path tracking and yaw control.

SMC has also been applied to differential braking systems, exploiting its robustness against disturbances and parameter uncertainties. Reference [22] introduced a phase-portrait-based SMC method that uses differential braking to maintain dynamic stability in car-trailer combinations. Similarly, Reference [23] implemented a multi-objective SMC algorithm for heavy tractor-semitrailers, focusing on jackknife prevention and yaw stability. Despite its robustness, SMC requires careful design to mitigate the chattering phenomenon, which can lead to actuator wear.

In addition, Fuzzy Logic Control has been employed to manage nonlinearities and uncertainties without relying on precise mathematical models. Reference [19] demonstrated that fuzzy logic can effectively generate additional yaw moments through differential braking, improving lateral stability under varying load conditions. Adaptive Control strategies have also been explored, adjusting braking torque in real time to compensate for changes in vehicle parameters such as payload or road friction. Reference [26] analyzed active trailer differential braking using adaptive control to prevent instability during dynamic maneuvers.

Recent research emphasizes Integrated Multi-System Control, which combines differential braking with other actuators such as active front steering and torque vectoring. Reference [28] proposed a coordinated control strategy for distributed-drive articulated trucks, combining differential braking with steering interventions to enhance anti-jackknifing stability. Reference [24] also investigated integrated control schemes that leverage both braking and steering for comprehensive yaw motion management.

Across all these approaches, a key finding emerges: tractor-only braking provides effective yaw control but limited trailer stabilization [1,23], while trailer-only braking directly mitigates trailer sway but lacks influence on tractor dynamics [28,29,34]. Coordinated braking on both units delivers optimal stability, reducing articulation angle and yaw rate deviations under critical speed conditions [14,15,19,22]. These results confirm that differential braking, when combined with advanced control strategies, is a cornerstone for achieving safe and reliable autonomous operation of articulated vehicles. These results are summarized in Table 4.

Table 4. Comparative effectiveness of braking configurations for yaw and sway stability.

Configuration	Studies	Findings
Tractor only	[1,23]	Effective for yaw control but limited trailer influence
Trailer only	[26,28,29,34]	Direct trailer stabilization, effective for sway control
Both units	[14,15,19,22]	Superior performance, comprehensive stability control

Finally, driver assistance systems and training complement these technologies. But, in the context of autonomous driving, the role of driver assistance systems evolves into fully integrated automated control architectures that replace human intervention entirely. Traditional features such as adaptive cruise control and lane-keeping assist become foundational components of advanced autonomous systems, which incorporate real-time sensor fusion, predictive algorithms, and coordinated braking strategies to maintain stability under dynamic conditions. These systems can continuously monitor articulation angles, yaw rates, and lateral accelerations, applying corrective actions such as differential braking and active trailer sway control without relying on driver input. Furthermore, machine learning-based predictive stability controllers can anticipate critical scenarios—such as

sudden lane changes or low-friction surfaces—and adjust braking forces across tractor and trailer axles to prevent jackknifing or swing.

The transition from driver assistance to full autonomy eliminates the variability associated with human decision-making and reaction times, enabling precise, coordinated interventions that optimize safety margins. However, this shift requires robust redundancy in sensing and actuation systems, as well as fail-safe algorithms to handle sensor degradation or unexpected environmental conditions. Ultimately, the integration of advanced stability control strategies—such as electronic stability control, differential braking, and active sway mitigation—into autonomous platforms is a cornerstone for achieving reliable and safe operation of articulated vehicles in mixed traffic environments.

1.2. Research Objectives and Proposed Solution

As previously mentioned, although numerous studies have addressed articulated vehicle stability, most existing approaches either provide reactive interventions or focus on single objectives such as yaw control or trajectory tracking. Conventional systems like ESC and RSC lack predictive capability, and advanced methods such as Fuzzy Logic and Sliding Mode Control face limitations in handling multi-variable constraints and ensuring proactive control under high-speed or autonomous conditions. This gap is particularly critical for next-generation heavy-duty vehicles, which must guarantee stability without human intervention.

The transition toward fully autonomous articulated vehicles requires control systems that go beyond conventional stability interventions. Existing studies employing MPC for yaw stability primarily focus on mitigating articulation angle deviations or preventing jackknifing through differential braking or steering coordination [14–16]. While these approaches demonstrate the predictive capability of MPC and its effectiveness in handling multi-variable constraints, they generally address stability as an isolated objective and do not explicitly regulate longitudinal speed to maintain safe operating conditions.

To overcome these limitations, this paper proposes an MPC-based control strategy that integrates trajectory tracking, yaw stability, and longitudinal speed regulation within a unified optimization framework, using differential braking as the primary actuator. The main objective is to provide a more anticipatory form of stability control and improve overall dynamic behavior, highlighting MPC as a practical option for enhancing the safety and reliability of autonomous articulated vehicles.

The core innovation lies in combining yaw stability control with coordinated regulation of vehicle speed and steering angle—parameters inherently managed by autonomous driving systems. This holistic approach ensures that articulation stability is maintained during critical situations such as sudden lane changes, emergency braking, and low-friction surfaces. Differential braking, which applies unequal braking forces to individual wheels to generate corrective yaw moments, serves as the primary mechanism for stabilizing the articulated configuration under dynamic conditions.

Unlike previous works, which intervene only when instability is imminent, the proposed controller proactively manages vehicle dynamics by predicting future states and applying corrective actions in real time. Differential braking serves as the primary actuator for yaw control, while speed regulation ensures that the vehicle remains within stability limits even under high-speed or aggressive maneuvers.

Ultimately, the main contribution of this work is to provide “intelligence” to articulated vehicles, transforming them into fully autonomous systems capable of safe and reliable operation. Through detailed modeling and simulation, we demonstrate the effectiveness of the proposed MPC-based control strategy and outline directions for future experimental validation.

This dual capability—stability preservation and speed management—represents a significant advancement over existing MPC-based solutions. By embedding longitudinal velocity control into the optimization problem, the system not only prevents instability but also optimizes overall dynamic performance, positioning it as a key enabler for safe and reliable autonomous operation of articulated vehicles.

The remainder of this paper is organized as follows. Section 2 introduces the dynamic model of the articulated vehicle, including the assumptions and governing equations as well as the details of the design of the MPC-based control system. Section 3 presents the simulation results for different operating conditions, illustrating the effectiveness of the proposed approach. Section 4 provides a discussion of the findings in the context of previous research and highlights their implications for autonomous driving. Finally, Section 5 summarizes the main conclusions and outlines directions for future work.

2. Materials and Methods

This section describes the modeling and control framework developed for this study. It begins with the formulation of a dynamic model representing the tractor–semitrailer combination, including the assumptions, degrees of freedom, and governing equations that capture the vehicle's kinematic and dynamic behavior. Subsequently, the design of the MPC system is presented, detailing the optimization problem, constraints, and cost function that integrate trajectory tracking, yaw stability, and longitudinal speed regulation. This section establishes the foundation for the simulation-based validation of the proposed control strategy.

2.1. Dynamic Model

The vehicle model is composed by two bodies, tractor and semitrailer, connected with an ideal revolute joint in the kingpin. The vehicle has two axles in the tractor and three axles in the semi-trailer and has been simplified by grouping the three semi-trailer axles in only one equivalent. Each axle has its equivalent left and right wheels. The truck has the driving system in the tractor rear axle, meanwhile the steering is applied in the front wheels.

A planar (yaw-plane) model of the tractor–semitrailer in which wheels and axles are represented by equivalent single-track groups has been adopted. This formulation is widely used for analyzing and controlling lateral/yaw stability in articulated combinations, with analytical and experimental support [1,5,35,36]. For stability-control design, capturing the yaw dynamics, articulation angle, and sideslip is sufficient; explicit roll degrees of freedom can be omitted without materially affecting the control objective of suppressing snaking/jackknife near the critical yaw speed [1,5]. Moreover, rollover is governed by the Static Rollover Threshold (SRT) defined in terms of lateral acceleration, and for the radii and maneuvers considered here, the speeds associated with reaching SRT are typically higher than those that trigger yaw-plane instabilities at comparable curvature; therefore, a planar model is appropriate for the lateral stability-control problem addressed in this study [37–39].

Therefore, with these assumptions, the vehicle model consists of a 2D model with 4 degrees of freedom, corresponding to the longitudinal and lateral displacements of the tractor, the tractor yaw angle and the semi-trailer yaw angle.

Figure 2 shows the vehicle schematics and the parameters considered in the model. The values of the parameters used in the model are relegated to Appendix A.

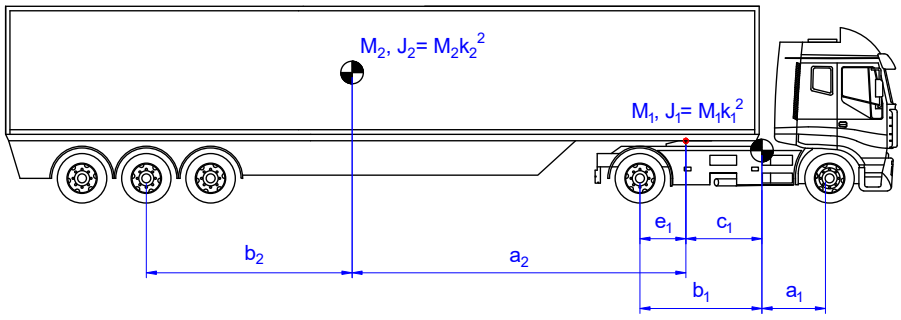

Figure 2. Model vehicle parameters.

A global inertial reference frame $\begin{bmatrix} X & Y \end{bmatrix}$ and two local reference frames $\begin{bmatrix} x_1 & y_1 \end{bmatrix}$ and $\begin{bmatrix} x_2 & y_2 \end{bmatrix}$ are defined. The tractor is represented as the body 1 and uses subscript 1 and the semitrailer is represented with subscript 2. Figure 3 shows the model variables.

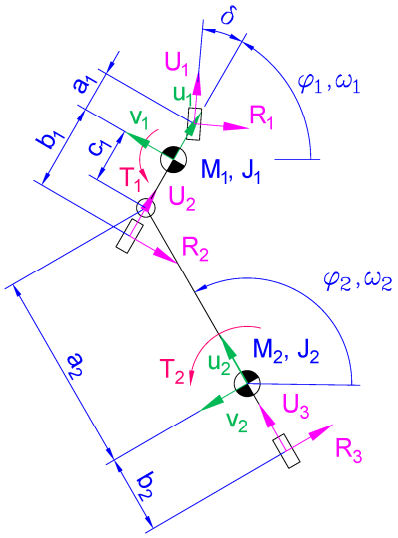

Figure 3. System variables definition.

To maintain consistency and clarity throughout the manuscript, the following notation conventions are adopted. All variables are written in italic type. Boldface characters denote vector and matrix quantities, whereas scalar quantities appear in regular (non-bold) type. Capital letters refer to variables expressed in the global reference frame, while lowercase letters refer to variables expressed in the local reference frame. Greek letters are used exclusively to represent rotational variables. These conventions are applied uniformly across equations, figures, and algorithmic descriptions.

The notation is defined as follows:

$\begin{bmatrix} X_i & Y_i \end{bmatrix}$ with $i = 1, 2$ are the c.o.g. (center of gravity) positions referred to the inertial reference frame $\begin{bmatrix} X & Y \end{bmatrix}$ for each body.

$\begin{bmatrix} u_i & v_i \end{bmatrix}$ with $i = 1, 2$ are the c.o.g. velocities referred to the local reference frame.

φ_i with $i = 1, 2$ are the orientation of the local reference frame with respect to the inertial reference frame.

φ_{ij} means $\varphi_i - \varphi_j$

$s\varphi_i$ means $sin\varphi_i$

$c\varphi_i$ means $cos\varphi_i$

$s\varphi_{ij}$ means $sin(\varphi_i - \varphi_j)$

$c\varphi_{ij}$ means $cos(\varphi_i - \varphi_j)$

ω_i with $i = 1, 2$ are the tractor and semitrailer yaw velocities.
ω_{ij} means $\omega_i - \omega_j$
$\boldsymbol{X} = \begin{bmatrix} X_1 & Y_1 & \varphi_1 & X_2 & Y_2 & \varphi_2 \end{bmatrix}^T$ is the vector of coordinates that represent the system movement in the inertial frame.
$\boldsymbol{V} = \begin{bmatrix} V_{x1} & V_{y_1} & \omega_1 & V_{x2} & V_{x2} & \omega_2 \end{bmatrix}^T$ is the vector of the c.o.g. velocities referred to the inertial frames.
$\boldsymbol{v} = \begin{bmatrix} u_1 & v_1 & \omega_1 & u_2 & v_2 & \omega_2 \end{bmatrix}^T$ is the vector of the c.o.g. velocities referred to the local frames.
$\boldsymbol{\lambda} = \begin{bmatrix} \lambda_x & \lambda_y \end{bmatrix}^T$ represents the constraint forces at the revolute joint, written in the global reference frame.
$\boldsymbol{F_e} = \begin{bmatrix} Fx_1 & Fy_1 & N_1 & Fx_2 & Fy_2 & N_2 \end{bmatrix}^T$ with i = 1, 2 (tractor, semitrailer) are resultant forces and momentum at the center of gravity (c.o.g.).
$\begin{bmatrix} U_1 & U_2 & U_3 \end{bmatrix}$ are the driving/braking forces in the front trailer axle, rear trailer axle and semitrailer axle.
$\begin{bmatrix} R_1 & R_2 & R_3 \end{bmatrix}$ represent the lateral tire forces in the front trailer axle, rear trailer axle and semitrailer axle.
$\begin{bmatrix} T_1 & T_2 \end{bmatrix}$ are the stability controllers, introduced as differential braking corresponding to the tractor and semitrailer, respectively, explained in Section 2.1.
$[\delta]$ represents the tractor steering angle.

In this paper, the individual axles of the tractor and the semitrailer are grouped into three axle sets: (i) the tractor's front axle, identified by subscript 1; (ii) the tractor's rear driving assembly—comprising the two driving wheels (or, where applicable, the tandem drive axles)—identified by subscript 2; and (iii) the three axles of the semitrailer, identified by subscript 3. Hereafter, any variable associated with each group is denoted using the corresponding subscript, as is the case with $\begin{bmatrix} U_1 & U_2 & U_3 \end{bmatrix}$ and $\begin{bmatrix} R_1 & R_2 & R_3 \end{bmatrix}$.

On the other hand, the variables T_1 and T_2 represent the yaw moments applied to the tractor and semitrailer, respectively, as part of the differential braking strategy. These yaw moments are generated by applying two equal and opposite braking forces on the left and right wheels of the same axle. Because these forces are symmetric and act in opposite directions, they do not produce any net longitudinal braking force on the vehicle; however, they create a pure yaw torque that influences the rotational dynamics of the corresponding unit. This formulation isolates the yaw-control effect of differential braking, ensuring that the generated torque influences only the rotational dynamics without introducing any net longitudinal deceleration to the vehicle.

The system equations can be obtained by applying the Newton-Euler' Laws for a multibody system with kinematic constraints. These equations are obtained in the local reference frame for both bodies and can be arranged in a matrix Formulation (1):

$$\boldsymbol{M} \cdot \left(\dot{\boldsymbol{v}} + \boldsymbol{v} \times \boldsymbol{\omega} \right) + \boldsymbol{A} \cdot \boldsymbol{\lambda} = \boldsymbol{F_e} \tag{1}$$

being

$$\boldsymbol{M} = \begin{bmatrix} M_1 & 0 & 0 & 0 & 0 & 0 \\ 0 & M_1 & 0 & 0 & 0 & 0 \\ 0 & 0 & J_1 & 0 & 0 & 0 \\ 0 & 0 & 0 & M_2 & 0 & 0 \\ 0 & 0 & 0 & 0 & M_2 & 0 \\ 0 & 0 & 0 & 0 & 0 & J_2 \end{bmatrix} \tag{2}$$

and, because $\boldsymbol{v}$ is in local Frames (3),

$$\dot{\boldsymbol{v}} + \boldsymbol{v} \times \boldsymbol{\omega} = \begin{bmatrix} \dot{u}_1 - v_1\omega_1 \\ \dot{v}_1 + u_1\omega_1 \\ \dot{\omega}_1 \\ \dot{u}_2 - v_2\omega_2 \\ \dot{v}_2 + u_2\omega_2 \\ \dot{\omega}_2 \end{bmatrix} \tag{3}$$

Equation (1) include also the vector $\boldsymbol{\lambda}$ with two additional variables that represent the two constraint forces at the revolute joint.

The expression of the constraint equations, written in terms of velocities in the inertial frame, is as follows (4):

$$\begin{bmatrix} 1 & 0 & c_1\, s\varphi_1 & -1 & 0 & a_2\, s\varphi_2 \\ 0 & 1 & -c_1\, s\varphi_1 & 0 & -1 & -a_2\, s\varphi_2 \end{bmatrix} \begin{bmatrix} V_{x1} \\ V_{y_1} \\ \omega_1 \\ V_{x2} \\ V_{y_2} \\ \omega_2 \end{bmatrix} = \begin{bmatrix} 0 \\ 0 \end{bmatrix} \tag{4}$$

And considering that:

$$\begin{bmatrix} V_{x1} \\ V_{y_1} \\ \omega_1 \\ V_{x2} \\ V_{y_2} \\ \omega_2 \end{bmatrix} = \begin{bmatrix} c\varphi_1 & -s\varphi_1 & 0 & 0 & 0 & 0 \\ s\varphi_1 & c\varphi_1 & 0 & 0 & 0 & 0 \\ 0 & 0 & 1 & 0 & 0 & 0 \\ 0 & 0 & 0 & c\varphi_2 & -s\varphi_2 & 0 \\ 0 & 0 & 0 & s\varphi_2 & c\varphi_2 & 0 \\ 0 & 0 & 0 & 0 & 0 & 1 \end{bmatrix} \begin{bmatrix} u_1 \\ v_1 \\ \omega_1 \\ u_2 \\ v_2 \\ \omega_2 \end{bmatrix} \tag{5}$$

The matrix $\boldsymbol{A}$ in (1) has the following expression (6):

$$\boldsymbol{A} = \begin{bmatrix} c\varphi_1 & s\varphi_1 \\ -s\varphi_1 & c\varphi_1 \\ c_1 s\varphi_1 & -c_1 c\varphi_1 \\ -c\varphi_2 & s\varphi_2 \\ -s\varphi_2 & -c\varphi_2 \\ a_2 s\varphi_2 & -a_2 s\varphi_2 \end{bmatrix} \tag{6}$$

Moreover, to know the position in global coordinates, it is necessary to add the following Equation (7):

$$\begin{bmatrix} \dot{X}_1 \\ \dot{Y}_1 \\ \dot{\varphi}_1 \\ \dot{X}_2 \\ \dot{Y}_2 \\ \dot{\varphi}_2 \end{bmatrix} = \begin{bmatrix} c\varphi_1 & -s\varphi_1 & 0 & 0 & 0 & 0 \\ s\varphi_1 & c\varphi_1 & 0 & 0 & 0 & 0 \\ 0 & 0 & 1 & 0 & 0 & 0 \\ 0 & 0 & 0 & c\varphi_2 & -s\varphi_2 & 0 \\ 0 & 0 & 0 & s\varphi_2 & c\varphi_2 & 0 \\ 0 & 0 & 0 & 0 & 0 & 1 \end{bmatrix} \begin{bmatrix} u_1 \\ v_1 \\ \omega_1 \\ u_2 \\ v_2 \\ \omega_2 \end{bmatrix} \tag{7}$$

And the constraint equations written in terms of velocities in the local frame, become as (8):

$$\begin{bmatrix} c\varphi_1 & -s\varphi_1 & c_1 s\varphi_1 & -c\varphi_2 & -s\varphi_2 & a_2\, s\varphi_2 \\ s\varphi_1 & c\varphi_1 & -c_1\, s\varphi_1 & s\varphi_2 & -c\varphi_2 & -a_2\, s\varphi_2 \end{bmatrix} \begin{bmatrix} u_1 \\ v_1 \\ \omega_1 \\ u_2 \\ v_2 \\ \omega_2 \end{bmatrix} = \begin{bmatrix} 0 \\ 0 \end{bmatrix} \tag{8}$$

Then, the equations that define the vehicle dynamics (9) are a set of six differential equations in terms of accelerations (1), six differential equations in terms of velocities (7), and two algebraic equations (8).

$$\begin{bmatrix} M_1 & 0 & 0 & 0 & 0 & 0 \\ 0 & M_1 & 0 & 0 & 0 & 0 \\ 0 & 0 & J_1 & 0 & 0 & 0 \\ 0 & 0 & 0 & M_2 & 0 & 0 \\ 0 & 0 & 0 & 0 & M_2 & 0 \\ 0 & 0 & 0 & 0 & 0 & J_2 \end{bmatrix} \begin{bmatrix} \dot{u}_1 - v_1\omega_1 \\ \dot{v}_1 + u_1\omega_1 \\ \dot{\omega}_1 \\ \dot{u}_2 - v_2\omega_2 \\ \dot{v}_2 + u_2\omega_2 \\ \dot{\omega}_2 \end{bmatrix} + \begin{bmatrix} c\varphi_1 & s\varphi_1 \\ -s\varphi_1 & c\varphi_1 \\ c_1 s\varphi_1 & -c_1 c\varphi_1 \\ -c\varphi_2 & s\varphi_2 \\ -s\varphi_2 & -c\varphi_2 \\ a_2 s\varphi_2 & -a_2 s\varphi_2 \end{bmatrix} \begin{bmatrix} \lambda_x \\ \lambda_y \end{bmatrix} = \begin{bmatrix} Fx_1 \\ Fy_1 \\ N_1 \\ Fx_2 \\ Fy_2 \\ N_2 \end{bmatrix}$$

$$\begin{bmatrix} \dot{X}_1 \\ \dot{Y}_1 \\ \dot{\varphi}_1 \\ \dot{X}_2 \\ \dot{Y}_2 \\ \dot{\varphi}_2 \end{bmatrix} = \begin{bmatrix} c\varphi_1 & -s\varphi_1 & 0 & 0 & 0 & 0 \\ s\varphi_1 & c\varphi_1 & 0 & 0 & 0 & 0 \\ 0 & 0 & 1 & 0 & 0 & 0 \\ 0 & 0 & 0 & c\varphi_2 & -s\varphi_2 & 0 \\ 0 & 0 & 0 & s\varphi_2 & c\varphi_2 & 0 \\ 0 & 0 & 0 & 0 & 0 & 1 \end{bmatrix} \begin{bmatrix} u_1 \\ v_1 \\ \omega_1 \\ u_2 \\ v_2 \\ \omega_2 \end{bmatrix} \tag{9}$$

$$\begin{bmatrix} c\varphi_1 & -s\varphi_1 & c_1 s\varphi_1 & -c\varphi_2 & -s\varphi_2 & a_2\, s\varphi_2 \\ s\varphi_1 & c\varphi_1 & -c_1\, s\varphi_1 & s\varphi_2 & -c\varphi_2 & -a_2\, s\varphi_2 \end{bmatrix} \begin{bmatrix} u_1 \\ v_1 \\ \omega_1 \\ u_2 \\ v_2 \\ \omega_2 \end{bmatrix} = \begin{bmatrix} 0 \\ 0 \end{bmatrix}$$

These differential-algebraic equations can be optimized and reduced to a minimum set of differential equations as a function of just the degrees of freedom of the system by eliminating the algebraic constraints, as shown in [40].

Then, two dependent velocities can be eliminated, and Equations (1) and (5) will be expressed only in terms of four independent velocities. In this case the dependent velocities chosen are the semi-trailer velocities (u_2 v_2).

In order to do so, it is necessary to define a matrix $\boldsymbol{S}$, that projects all the velocities to the independent ones. This matrix can be written as:

$$\boldsymbol{S} = \begin{bmatrix} 1 & 0 & 0 & 0 \\ 0 & 1 & 0 & 0 \\ 0 & 0 & 1 & 0 \\ c\varphi_{12} & -s\varphi_{12} & c_1 s\varphi_{12} & 0 \\ s\varphi_{12} & c\varphi_{12} & -c_1 c\varphi_{12} & -a_2 \\ 0 & 0 & 0 & 1 \end{bmatrix} \tag{10}$$

Then:

$$\begin{bmatrix} u_1 \\ v_1 \\ \omega_1 \\ u_2 \\ v_2 \\ \omega_2 \end{bmatrix} = \boldsymbol{S} \begin{bmatrix} u_1 \\ v_1 \\ \omega_1 \\ \omega_2 \end{bmatrix} \tag{11}$$

And

$$\begin{bmatrix} \dot{u}_1 \\ \dot{v}_1 \\ \dot{\omega}_1 \\ \dot{u}_2 \\ \dot{v}_2 \\ \dot{\omega}_2 \end{bmatrix} = \dot{\boldsymbol{S}} \begin{bmatrix} u_1 \\ v_1 \\ \omega_1 \\ \omega_2 \end{bmatrix} + \boldsymbol{S} \begin{bmatrix} \dot{u}_1 \\ \dot{v}_2 \\ \dot{\omega}_1 \\ \dot{\omega}_2 \end{bmatrix} \tag{12}$$

Finally, substituting (12) into (1) and (7), and multiplying beforehand S^T, results in (13) and (14):

$$\begin{aligned} &\begin{bmatrix} M_1+M_2 & 0 & 0 & -M_2a_2s\varphi_{12} \\ 0 & M_1+M_2 & -M_2c_1 & -M_2a_2c\varphi_{12} \\ 0 & -M_2f & J_1+M_2fc_1{}^2 & M_2a_2c_1c\varphi_{12} \\ -M_2a_2s\varphi_{12} & -M_2a_2c\varphi_{12} & M_2a_2c_1c\varphi_{12} & J_2+M_2a_2{}^2 \end{bmatrix} \begin{bmatrix} \dot{u}_1 \\ \dot{v}_2 \\ \dot{\omega}_1 \\ \dot{\omega}_2 \end{bmatrix} = \\ &= \begin{bmatrix} 0 & M_1\omega_1+M_2(\omega_1+\omega_{12}) & -M_2c_1\omega_{12} & 0 \\ -M_1\omega_1-M_2(\omega_1+\omega_{12}) & 0 & 0 & 0 \\ M_2c_1\omega_1(\omega_1+\omega_{12}) & 0 & 0 & 0 \\ M_2a_2c\varphi_{12}(\omega_1+\omega_{12}) & -M_2a_2s\varphi_{12}(\omega_1+\omega_{12}) & M_2a_2c_1\omega_{12}s\varphi_{12} & 0 \end{bmatrix} \begin{bmatrix} u_1 \\ v_1 \\ \omega_1 \\ \omega_2 \end{bmatrix} \\ &+ \begin{bmatrix} Fx_1+Fx_2c\varphi_{12}+Fy_2s\varphi_{12} \\ Fy_1-Fx_2s\varphi_{12}+Fy_2c\varphi_{12} \\ N_1+Fx_2c_1s\varphi_{12}-Fy_2c_1c\varphi_{12} \\ -a_2Fy_2+N_2 \end{bmatrix} \end{aligned} \tag{13}$$

$$\begin{bmatrix} \dot{X}_1 \\ \dot{Y}_1 \\ \dot{\varphi}_1 \\ \dot{\varphi}_2 \end{bmatrix} = \begin{bmatrix} c\varphi_1 & -s\varphi_1 & 0 & 0 \\ s\varphi_1 & c\varphi_1 & 0 & 0 \\ 0 & 0 & 1 & 0 \\ 0 & 0 & 0 & 1 \end{bmatrix} \begin{bmatrix} u_1 \\ v_1 \\ \omega_1 \\ \omega_2 \end{bmatrix} \tag{14}$$

There are two types of forces and torques acting on the tractor-trailer combination.

On the one hand, $\begin{bmatrix} U_1 & U_2 & U_3 \end{bmatrix}$ are the driving/braking forces in the front trailer axle, rear trailer axle, and semitrailer axle. In the vehicle under study, tractive effort is provided exclusively by the tractor's rear drive assembly (U_2). By contrast, all three axle groups—U_1, U_2, and U_3—are equipped with braking capability. Therefore, when the vehicle is braking, all of them are brake forces. However, when the truck is accelerating, only U_2 is active.

Conversely, $\begin{bmatrix} R_1 & R_2 & R_3 \end{bmatrix}$ denotes the cornering tire forces exerted by the front trailer axle, rear trailer axle, and semitrailer axle.

The driving/braking forces are applied in the longitudinal direction of the tires, whilst the cornering tire forces are applied in the lateral direction of the tires, so the contribution to the general forces vector is shown in (15).

Finally, are the stability controllers $\begin{bmatrix} T_1 & T_2 \end{bmatrix}$ are introduced as inputs coming from the controller in the form of torques applied the tractor and in the semi-trailer. Differential braking means that an equal and opposite increase in braking force is applied to the wheels

on each side of each axle, which means that there is no additional braking increase, but there is a torque that affects the yaw movement.

$$\begin{bmatrix} Fx_1 \\ Fy_1 \\ N_1 \\ Fx_2 \\ Fy_2 \\ N_2 \end{bmatrix} = \begin{bmatrix} U_1 \cos\delta + U_2 - R_1 \sin\delta \\ U_1 \sin\delta + R_1 \cos\delta + R_2 \\ R_1 a_1 \cos\delta - b_1\, R_2 + T_1 \\ U_3 \\ R_3 \\ -b_2\, R_3 + T_2 \end{bmatrix} \tag{15}$$

Lateral tire forces, R_i, are required to negotiate a curve. They result in tire slip angles. This tire characteristic is linear for small slip angles. The gradient of the curve in the linear regime is the tire cornering stiffness, C_i.

A normalized cornering stiffness is used to study the effect of scaling the tire cornering stiffness linearly with vertical load on dynamic stability. It was found in [41] that, in contrast to passenger car tires, the relation between the tire cornering stiffness and vertical load is nearly linear for truck tires and that the characteristic shows an even more linear relationship if dual tires are applied, which is often the case in truck configurations, except for the steered axle.

This means that the assumption that the cornering stiffness versus load characteristic is in its linear region is often true for truck tires.

The cornering stiffnesses are calculated as function of vertical load, with $f = f_1 = f_2 = f_3 = 5.73$ [1/rad] using expressions in (16) and (17)

$$\begin{array}{ll} C_1 = f\, F_{Z1} & F_{Z1} = M_1 g \frac{b_1}{l_1} - M_2 g \frac{b_2}{l_2} \frac{e_1}{l_1} \\ C_2 = f\, F_{Z2} & F_{Z2} = M_1 g \frac{a_1}{l_1} + M_2 g \frac{b_2}{l_2} \frac{l_{1s}}{l_1} \\ C_3 = f\, F_{Z3} & F_{Z3} = M_2 g \frac{a_2}{l_2} \end{array} \tag{16}$$

with:

$$\begin{aligned} l_1 &= a_1 + b_1 \\ l_2 &= a_2 + b_2 \\ l_{1s} &= a_1 + b_1 + e_1 \end{aligned} \tag{17}$$

The lateral tire forces R_i are obtained from the slip angle α_i, that depends on the relation between the lateral and longitudinal wheel speed on the ground contact point, according to the following expressions (18) by multiplying the slip angle by the cornering stiffness C_i:

$$\begin{array}{ll} R_1 = C_1 \alpha_1 & \alpha_1 = (v_1 + a_1 \omega_1)/u_1 - \delta \\ R_2 = C_2 \alpha_2 & \alpha_2 = (v_1 - b_1 \omega_1)/u_1 \\ R_3 = C_3 \alpha_3 & \alpha_3 = (v_2 - b_2 \omega_2)/u_2 \end{array} \tag{18}$$

The model assumes small steering angles, so $\sin\delta \cong \delta$ and $\cos\delta \cong 1$.

Then, the final equations result as in (19)

$$\begin{bmatrix} M_1+M_2 & 0 & 0 & -M_2\,a_2\,s\varphi_{12} \\ 0 & M_1+M_2 & -M_2c_1 & -M_2\,a_2\,c\varphi_{12} \\ 0 & -M_2f & J_1+M_2{f{c_1}^2} & M_2\,a_2\,c_1\,c\varphi_{12} \\ -M_2\,a_2\,s\varphi_{12} & -M_2\,a_2\,c\varphi_{12} & M_2\,a_2\,c_1\,c\varphi_{12} & J_2+M_2{a_2}^2 \end{bmatrix} \begin{bmatrix} \dot{u}_1 \\ \dot{v}_2 \\ \dot{\omega}_1 \\ \dot{\omega}_2 \end{bmatrix} =$$
$$= \begin{bmatrix} 0 & M_1\omega_1+M_2(\omega_1+\omega_{12}) & -M_2c_1\omega_{12} & 0 \\ -M_1\omega_1-M_2(\omega_1+\omega_{12}) & 0 & 0 & 0 \\ M_2c_1\omega_1(\omega_1+\omega_{12}) & 0 & 0 & 0 \\ M_2a_2c\varphi_{12}(\omega_1+\omega_{12}) & -M_2a_2s\varphi_{12}(\omega_1+\omega_{12}) & M_2a_2c_1\omega_{12}\,s\varphi_{12} & 0 \end{bmatrix} \begin{bmatrix} u_1 \\ v_1 \\ \omega_1 \\ \omega_2 \end{bmatrix} \quad (19)$$
$$+ \begin{bmatrix} U_1+U_2+U_3\,c\varphi_{12}-\delta\,R_1+R_3\,s\varphi_{12} \\ \delta\,U_1-U_3\,s\varphi_{12}+R_1+R_2+R_3\,c\varphi_{12} \\ U_3\,c_1\,s\varphi_{12}+R_1a_1-b_1\,R_2-R_3\,c_1\,c\varphi_{12}+T_1 \\ -(a_2+b_2)\,R_3+T_2 \end{bmatrix}$$
$$\begin{bmatrix} \dot{X}_1 \\ \dot{Y}_1 \\ \dot{\varphi}_1 \\ \dot{\varphi}_2 \end{bmatrix} = \begin{bmatrix} c\varphi_1 & -s\varphi_1 & 0 & 0 \\ s\varphi_1 & c\varphi_1 & 0 & 0 \\ 0 & 0 & 1 & 0 \\ 0 & 0 & 0 & 1 \end{bmatrix} \begin{bmatrix} u_1 \\ v_1 \\ \omega_1 \\ \omega_2 \end{bmatrix}$$

2.2. Design of the MPC Controller

This section presents the formulation of an optimization problem aimed at designing controllers that guide the vehicle and maintain yaw stability. The optimal control design is derived from the dynamic model of the trailer. The control inputs considered include the driving and braking forces at each axle, the steering angle, and the torque associated with differential braking for yaw stability control. Operational constraints are imposed by defining permissible limits for both inputs and outputs. Additionally, an objective function is introduced to capture the goals of the control problem: tracking a desired trajectory while ensuring yaw stability.

2.2.1. Optimal Control Design

Regrouping the previous expression (19) the system equations for the vehicle dynamics are written in a compacted way as (20):

$$\dot{\boldsymbol{x}} = f_v(\boldsymbol{x}, \boldsymbol{U}) \quad (20)$$

where

$\boldsymbol{x} = \begin{bmatrix} {V_I}^T & {X_i}^T \end{bmatrix}^T$ is a vector including the states.

$\boldsymbol{V_I} = \begin{bmatrix} u_1 & v_1 & \omega_1 & \omega_2 \end{bmatrix}^T$ is vector with the independent velocities.

$\boldsymbol{X_i} = \begin{bmatrix} X_1 & Y_1 & \varphi_1 & \varphi_2 \end{bmatrix}^T$ includes the global positions and orientations for tractor and semitrailer.

$\boldsymbol{U} = \begin{bmatrix} U_1 & U_2 & U_3 & \delta & T_1 & T_2 \end{bmatrix}^T$ is a vector including the inputs.

An MPC approach is proposed for the vehicle. MPC is selected due to its capability of systematically handling multiple input and state constraints, which in this problem are critical. According to the receding horizon principle, at each time step the MPC algorithm computes the optimal control and state trajectories solving a finite horizon optimization problem.

For the formulation of the MPC a prediction horizon $\left[t, t+N_p\right]$ is considered at time t. The notation $\boldsymbol{x}_{t+k|t}$ represents the state vector at time $t+k$, predicted at time t, obtained by starting from the current state $\boldsymbol{x}_{t|t} = \boldsymbol{x}(t) \equiv \boldsymbol{x}_t$, and where $\boldsymbol{U}_{\cdot|t} = \left[\boldsymbol{U}_{t|t}, \ldots, \boldsymbol{U}_{t+N_p-1|t}\right]$

denotes the unknown input variables to be optimized. As previously stated, the subscript 1 denotes the tractor and subscript 2 denotes the semitrailer.

2.2.2. System Dynamics

Equation (21) represents the system dynamics updates for the discrete-time model obtained from (20). The initial state is set in (22)

$$\begin{array}{c} \boldsymbol{x}_{k+1|t} = f\left(\boldsymbol{x}_{k|t}, \boldsymbol{U}_{k|t}\right) \\ \forall k = t, \ldots, t + N_p - 1 \end{array} \tag{21}$$

$$\boldsymbol{x}_{t|t} = \boldsymbol{x}_t \tag{22}$$

2.2.3. Constraints

The controlled inputs include the driving and braking forces at each axle, the steering angle, and the torque representing differential braking for yaw stability control.

The driving and braking forces must be bounded by:

$$-F_{b1} \leq U_{1k|t} \leq 0 \tag{23}$$

$$-F_{b2} \leq U_{2k|t} \leq F_{d2} \tag{24}$$

$$-F_{b3} \leq U_{3k|t} \leq 0 \tag{25}$$

$$\begin{array}{c} -P_b \leq u_{1k|t}\left(U_{1k|t} + U_{2k|t}\right) + u_{2k|t}U_{3k|t} \leq P_d \\ \forall k = t, \ldots, t + N_p - 1 \end{array} \tag{26}$$

The driving/braking forces constraints include the limitation of the maximum driving and braking force and the power limitation in driving and braking. Equations (23)–(26) represent the maximum driving/braking forces and the maximum power for driving/braking. Equations (23) and (25) are bounded between $[-F_{bi}, 0]$ because axles 1 and 3 only break, instead of axel 2 (24), bounded between $[-F_{b2}, F_{d2}]$ because in this axle, we have de traction.

Constraints (27) and (28) bounds the steering angle and the steering rate.

$$-\delta_{max} \leq \delta_{k|t} \leq \delta_{max} \tag{27}$$

$$\begin{array}{c} -\dot{\delta}_{max} \leq \left(\delta_{k|t} - \delta_{k-1|t}\right)\Delta t/ \leq \dot{\delta}_{max} \\ \forall k = t, \ldots, t + N_p - 1 \end{array} \tag{28}$$

And constraints (29) constraints the differential braking stability controllers

$$\begin{array}{c} -T_{1max} \leq T_1 \leq T_{1max} \\ -T_{2max} \leq T_2 \leq T_{2max} \end{array} \tag{29}$$

In the MPC formulation, we will refer to all these constraints as $u_{k|t} \in \mathbb{U}_{k|t}$.

In order to guarantee that the vehicle respects the speed limit, the speed is bounded by the following constraint (30):

$$\begin{array}{c} v_{min} \leq u_{1k|t} \leq v_{max} \\ \forall k = t, \ldots, t + N_p - 1 \end{array} \tag{30}$$

In the MPC, we will refer to this constraint as $v_{k|t} \in \mathbb{V}_{k|t}$.

2.2.4. Cost Function

The objective of the truck is to circulate at the speed fixed by a reference, following a trajectory previously define, and preserving yaw stability. The objective control may be stablished with an objective function composed by different terms. This objective function is used to minimize the different errors produced in the trajectory tracking and in the relative yaw rate, as shown in Figure 4.

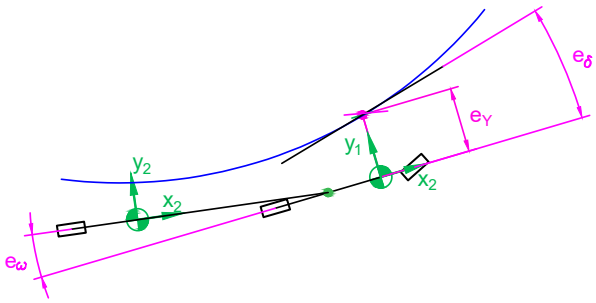

Figure 4. Errors to be minimized in the cost function.

Therefore, the objective function $J(\boldsymbol{x}, \boldsymbol{U})$ (31) is defined as follows:

$$J(\boldsymbol{x}, \boldsymbol{U}) = \sum_{k=t}^{t+N_p} K_V \left(u_{1k\,|\,t} - u_{ref} \right)^2 + \sum_{k=t}^{t+N_p} K_Y {e_Y}^2 + \sum_{k=t}^{t+N_p} K_\alpha {e_\delta}^2 + \sum_{k=t}^{t+N_p} K_\omega {e_\omega}^2 \tag{31}$$

with

$$e_Y = y_{1k|t} - Y_{roadk|t} \tag{32}$$

$$e_\delta = \varphi_{1k|t} - \alpha_{roadk|t} \tag{33}$$

$$e_\omega = \dot{\varphi}_{1k|t} - \dot{\varphi}_{2k|t} \tag{34}$$

The different terms in the cost function (31) to (34) have the following meaning: $K_V \geq 0$ represents the weight penalizing the output deviation from the truck maximum desired speed, being u_{ref} the maximum desired speed. $K_Y \geq 0$ represents the weight penalizing the lateral displacement in the trajectory tracking, being $Y_{k|t}$ the Y coordinate of the desired trajectory. $K_\alpha \geq 0$ represents the weight penalizing the orientation in the trajectory tracking being $\alpha_{k|t}$ the orientation of the desired trajectory.

The term (34) is the key point in the yaw stability control. This term minimizes the yaw rate between tractor and semitrailer, so it preserves the yaw instability.

2.2.5. Model Predictive Control Formulation

As previously said, the objective of the truck is to circulate at the speed fixed by a reference, following a trajectory previously define, and preserving yaw stability.

Therefore, the optimization problem is formulated as (35)–(39):

$$\min_{U_{\cdot|t}} J(\boldsymbol{x}, \boldsymbol{U}) \tag{35}$$

subject to:

$$\boldsymbol{x}_{k+1|t} = f\left(\boldsymbol{x}_{k|t}, \boldsymbol{U}_{k|t} \right) \tag{36}$$

$$\boldsymbol{U}_{k|t} \in \mathbb{U}_{k|t} \tag{37}$$

$$\begin{gathered} v_{k|t} \in \mathbb{V}_{k|t} \\ \forall k = t, \ldots, t + N_p - 1 \end{gathered} \tag{38}$$

$$x_{t|t} = x_t \tag{39}$$

The resulting optimal states and inputs of (35)–(39) are denoted as following:

$$\begin{aligned} \boldsymbol{x}_t^* &= \begin{pmatrix} x_{t\,|\,t}^* & x_{t+1\,|\,t}^* & \cdots & x_{t+N_p\,|\,t}^* \end{pmatrix}^T \\ \boldsymbol{U}_t^* &= \begin{pmatrix} U_{t\,|\,t}^* & U_{t+1\,|\,t}^* & \cdots & U_{t+N_p\,|\,t}^* \end{pmatrix}^T \end{aligned} \tag{40}$$

For closing the loop, the first input is applied to the system (20) during the time interval $[t, t+1]$

$$\boldsymbol{u}_t = \boldsymbol{u}_{t|t}^* \tag{41}$$

At the next time step $t+1$, a new optimal problem in the form of (35)–(39) is solved over a shifted horizon, based on a new states' measurement.

3. Results

Two different models have been developed for the design and validation of the yaw stability controller through simulation. The first model represents a trailer without a yaw stability controller, whereas the second model incorporates the stability controller. In the first model, term (34) of the cost function is not considered, while in the second model this term is introduced.

A velocity profile was defined following a sinusoidal path, as expressed in Equation (42):

$$\begin{aligned} Y_{road}(\mathrm{X}) &= 5 * \left(1 - \cos\left(\tfrac{\pi}{200}\mathrm{X}\right)\right) \\ \alpha_{road}(\mathrm{X}) &= \operatorname{atan}\left(5 * \tfrac{\pi}{200} \sin\left(\tfrac{\pi}{200}\mathrm{X}\right)\right) \end{aligned} \tag{42}$$

To evaluate the effectiveness of the proposed MPC-based control strategy, two simulation scenarios were analyzed: (i) a reference speed below the critical threshold (15 m/s) and (ii) a reference speed exceeding the critical threshold (35 m/s). The critical speed for the modeled tractor–semitrailer configuration was calculated as 31.04 m/s using the formulation in [5].

At a reference speed of 15 m/s, the articulated vehicle exhibits inherently stable behavior even without the yaw stability controller. Nevertheless, the implementation of the proposed MPC-based controller provides measurable improvements in articulation dynamics and trajectory tracking, as shown in Figures 5–7.

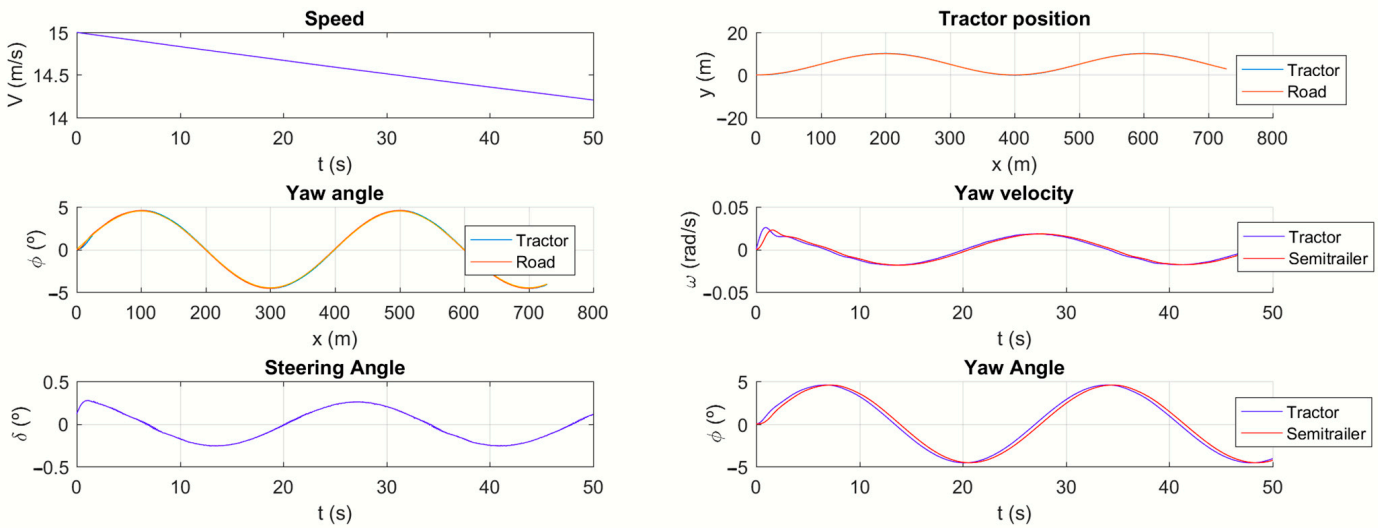

Figure 5. Trailer behavior without stability controller for v_{ref} = 15 m/s.

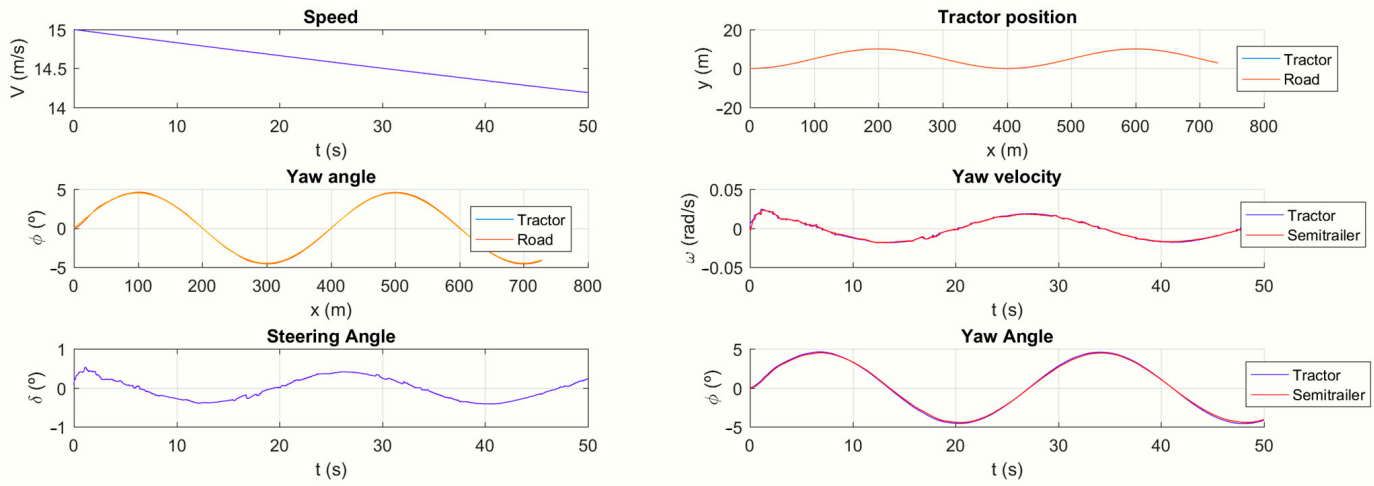

Figure 6. Trailer behavior with stability controller for v_{ref} = 15 m/s.

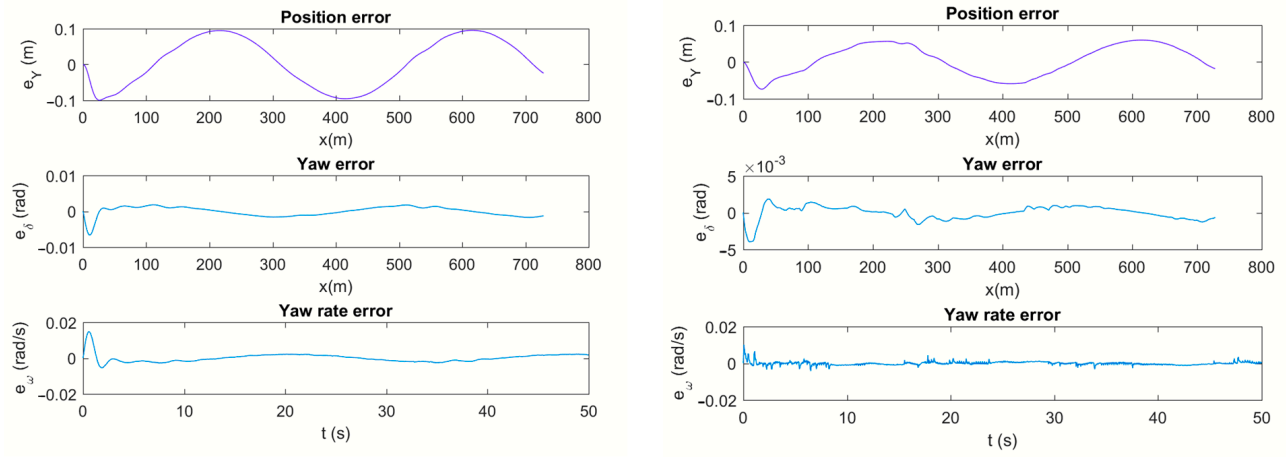

(**a**) Without yaw stability control (**b**) With yaw stability control

Figure 7. Tracking errors for v_{ref} = 15 m/s.

Figure 5 illustrates the trailer behavior without the stability controller, showing that the trailer remains stable and accurately tracks the desired trajectory. Figure 6 presents the trailer behavior with the stability controller activated. A comparison of these two figures indicates that, although the vehicle remains stable without the controller, the relative yaw angle between the tractor and semitrailer is slightly higher than in the case with the controller.

From Figure 7, the lateral position error remains below approximately 0.10 m without control and is further reduced to 0.06 m with control. Similarly, the yaw angle error decreases from about 0.006 rad to 0.004 rad, and the yaw rate error is reduced from 0.010 rad/s to 0.004 rad/s. These reductions, although moderate, confirm that the controller enhances maneuverability and coupling stability even under conditions where the system is naturally stable.

Conversely, at a reference speed of 35 m/s—well above the critical threshold—the uncontrolled vehicle exhibits severe instability, characterized by oscillatory yaw motion and significant trajectory deviation. Under these conditions, the trailer becomes unstable without the stability controller, as shown in Figures 8 and 9. Figure 8 illustrates that the trailer fails to track the desired trajectory, exhibiting oscillatory behavior before reducing its speed in an attempt to reach a stable velocity. Figure 9 presents the trailer behavior with the stability controller activated, demonstrating that the trailer remains stable throughout

the maneuver. Additionally, in the uncontrolled case, the trajectory tracking algorithm significantly reduces the vehicle's speed to below the critical threshold in an attempt to regain stability, whereas the MPC-based controller maintains the reference speed while preserving yaw stability and accurate path tracking. These results demonstrate the controller's ability to maintain stability and prevent jackknifing and trailer sway under extreme conditions.

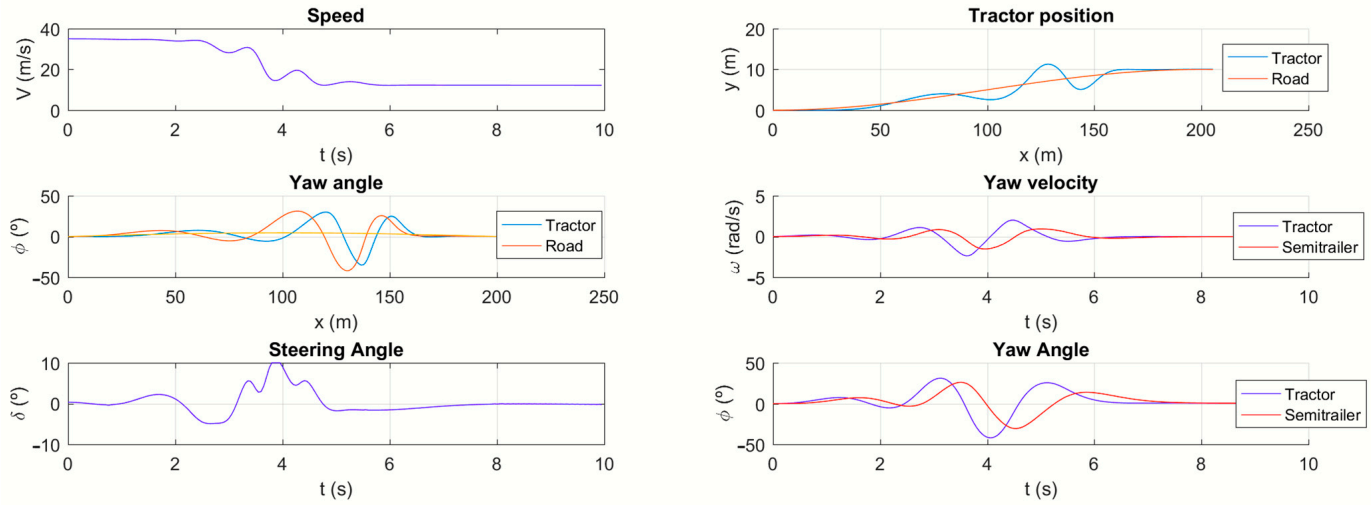

Figure 8. Trailer behavior without stability controller for v_{ref} = 35 m/s.

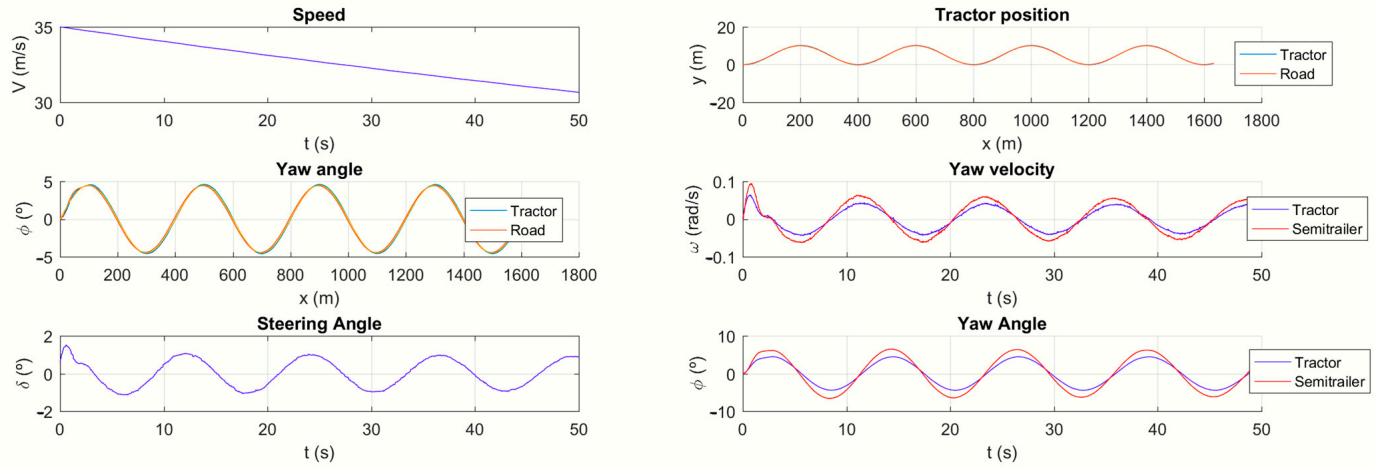

Figure 9. Trailer behavior with stability controller for v_{ref} = 35 m/s.

As shown in Figure 10, the lateral position error exceeds 5 m without control, while the MPC-based controller reduces this error to approximately 0.15 m, representing a substantial improvement. The yaw angle error decreases from 0.7 rad to 0.007 rad, and the yaw rate error drops from 4 rad/s to 0.025 rad/s. These results demonstrate the controller's ability to maintain stability and accurate path tracking under extreme conditions, confirming its effectiveness in preventing jackknifing and trailer sway at high speeds.

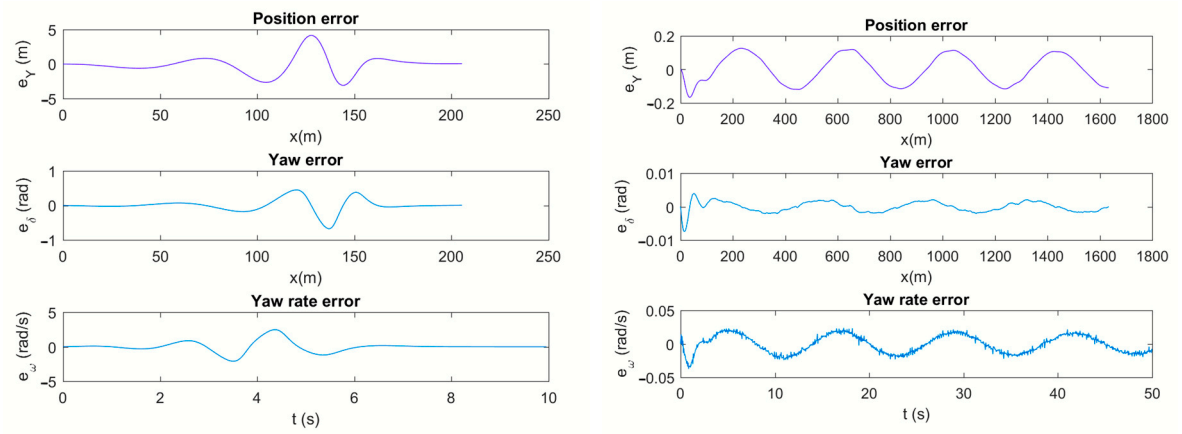

(**a**) Without yaw stability control (**b**) With yaw stability control

Figure 10. Tracking errors for v_{ref} = 35 m/s.

Figures 11 and 12 illustrate the trailer's motion under both stable and unstable conditions. The supplementary material includes Videos S1 and S2, which also illustrate this phenomenon.

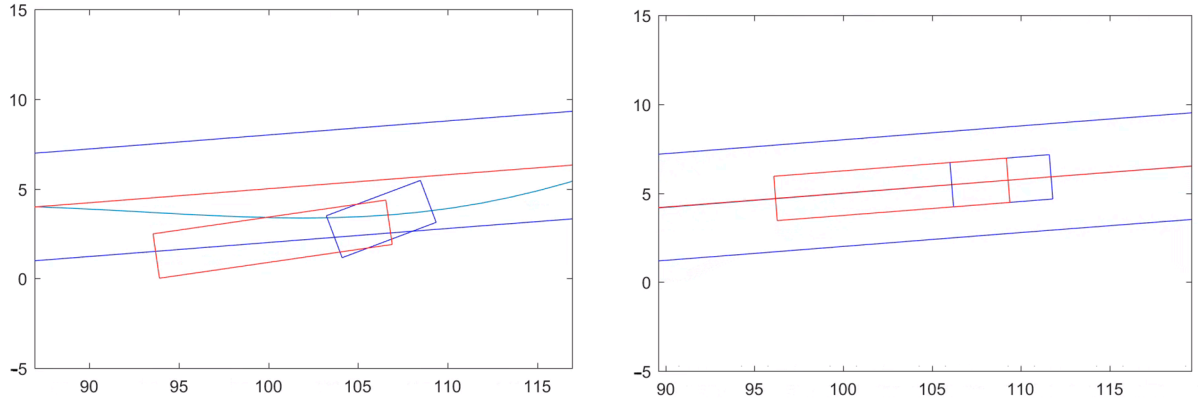

(**a**) Without yaw stability control (**b**) With yaw stability control

Figure 11. Pictures of the trailer movement for v_{ref} = 35 m/s.

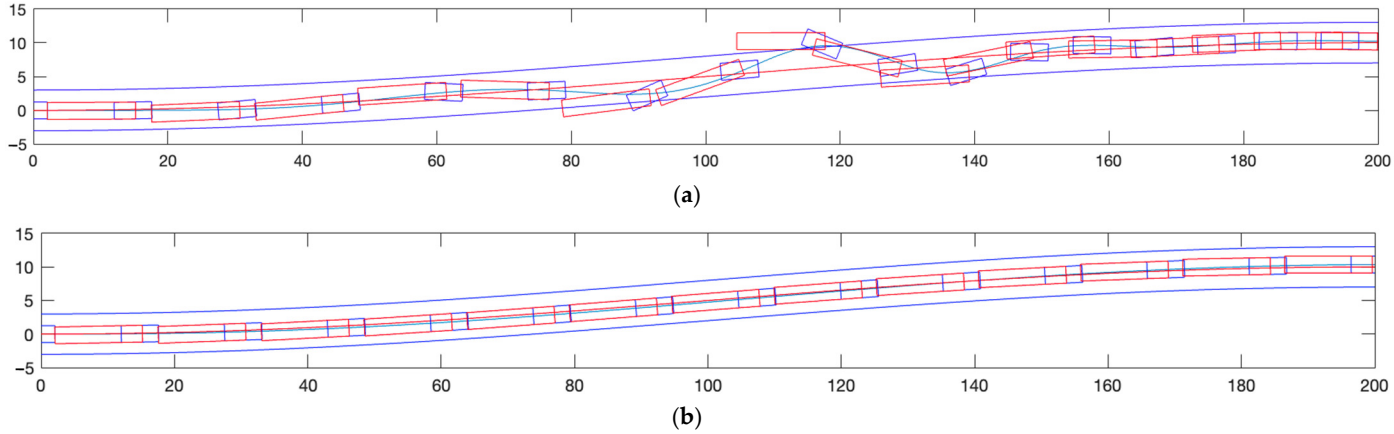

(**a**)

(**b**)

Figure 12. Different positions of the trailer movement for v_{ref} = 35 m/s. (**a**) Without yaw stability control; (**b**) With yaw stability control.

4. Discussion

The results obtained in this study highlight the advantages of MPC for stability management in autonomous articulated vehicles. Unlike conventional systems such as ESC or RSC, which intervene reactively after instability occurs, the MPC framework enables proactive control by predicting future states and optimizing actions over a receding horizon. This predictive capability is essential for managing nonlinear dynamics and multi-body interactions under high-speed and emergency conditions.

A key contribution of this work lies in the integration of yaw stability, trajectory tracking, and longitudinal speed regulation within a unified optimization framework. Previous studies have primarily addressed these objectives in isolation, focusing either on yaw stability or path tracking. By contrast, the proposed approach demonstrates that combining these objectives significantly improves overall dynamic performance. At moderate speeds (15 m/s), where the vehicle is inherently stable, the controller still reduces articulation angle and yaw rate deviations, enhancing maneuverability and reducing structural stress at the coupling point. These improvements, although modest, are relevant for autonomous operation in confined spaces or during lane changes, where precise articulation control is critical.

The benefits of the proposed strategy become more pronounced at high speeds (35 m/s), where instability phenomena such as jackknifing and trailer sway typically occur. Without active stability control, the vehicle exhibits oscillatory yaw motion and large trajectory deviations, ultimately reducing its speed below the critical threshold in an attempt to regain stability. In contrast, the MPC-based controller maintains the reference speed while preserving yaw stability and accurate path tracking. This dual capability—stabilizing yaw motion and regulating speed—represents a major advancement over existing MPC-based approaches, which generally neglect longitudinal velocity control. By actively managing speed, the controller prevents the onset of instability rather than merely reacting to it, ensuring safe operation under extreme conditions.

In addition to these findings, it is important to acknowledge the limitations of the current simulation campaign. The study focuses on two representative but dynamically contrasting operating conditions—moderate-speed operation at 15 m/s and extreme high-speed operation at 35 m/s—chosen deliberately to illustrate both stable and unstable regimes relative to the analytically derived critical speed. Although the high-speed case constitutes an extreme scenario from the standpoint of lateral and yaw dynamics, the overall test matrix remains limited in scope. The simulations are conducted under nominal assumptions, including flat road geometry, constant high friction, fixed payload conditions, and idealized brake actuation without explicit actuator or sensor dynamics. As a result, the results should be interpreted primarily as a proof-of-concept validation of the proposed control architecture rather than a full robustness study. Future work will expand the simulation space to include variations in friction, curvature, payload, and external disturbances, and will complement these simulations with hardware-in-the-loop experiments and full-scale testing to strengthen the reliability and generalizability of the findings.

Another important aspect is the use of differential braking as the primary actuator. This choice offers a cost-effective solution that leverages existing braking systems while providing sufficient yaw control authority. Coordinated braking across tractor and trailer units enhances corrective yaw moments and minimizes articulation deviations, contributing to improved safety margins. Although the present study assumes idealized brake actuation with negligible delay, future work will incorporate actuator dynamics and brake pressure response characteristics to evaluate real-time performance and guarantee control accuracy under practical conditions.

Overall, the findings confirm that MPC is not limited to preventing instability; it also optimizes vehicle dynamics for autonomous operation. By embedding predictive control, multi-objective optimization, and differential braking into a single framework, the proposed system addresses the fundamental challenges of articulated vehicle stability in a holistic manner. These capabilities position MPC as a cornerstone technology for next-generation heavy-duty autonomous vehicles.

Although the proposed control strategy has been evaluated through an extensive set of high-fidelity simulations, the present work does not yet include experimental testing. This limitation arises from the current stage of the project, in which the physical prototype and test bench are still under development. Future work will involve a comprehensive experimental validation campaign, including hardware-in-the-loop simulations and controlled full-scale tests. These experiments will be used to verify the controller's robustness, confirm its real-world performance, and refine the model-based assumptions introduced in this study.

5. Conclusions

The main contribution of this work lies in its holistic approach to articulated vehicle control, integrating trajectory tracking, yaw stability, and longitudinal speed regulation within a unified optimization framework. Unlike conventional stability systems that rely on reactive interventions, the proposed MPC-based strategy enables predictive, multi-objective control, addressing critical limitations in current technologies.

Simulation results under two representative scenarios confirm the effectiveness of the controller. At moderate speeds, the system improves articulation behavior and yaw dynamics, enhancing maneuverability even when the vehicle is inherently stable. At high speeds, where instability phenomena such as jackknifing and trailer sway typically occur, the controller maintains trajectory accuracy and yaw stability while preserving the reference speed—capabilities that conventional systems cannot achieve. These findings demonstrate that proactive speed regulation combined with differential braking significantly extends the operational safety envelope of articulated vehicles.

The use of differential braking as the primary actuator offers a practical and cost-effective solution, leveraging existing braking systems to generate corrective yaw moments without introducing additional longitudinal deceleration. Although the present study assumes idealized brake actuation and relies exclusively on simulation-based analysis due to the unavailability of a physical prototype at this stage, this approach allows for further exploration of extreme operating conditions that would be unsafe or impractical to reproduce experimentally. Future research will incorporate actuator dynamics, response delays, and multi-actuator coordination—including active steering and torque vectoring—while also progressing toward hardware-in-the-loop testing and full-scale experimental validation once the prototype becomes available.

Overall, the proposed MPC framework represents a substantial step toward reliable and safe autonomous operation of heavy-duty articulated vehicles. By combining predictive control, constraint handling, and integrated stability objectives, this approach provides a foundation for next-generation control architectures capable of meeting the stringent requirements of autonomous freight transportation. Additionally, the development of real-time optimization algorithms and fail-safe mechanisms will be critical for ensuring robustness and reliability in mixed traffic environments.

Supplementary Materials: The following supporting information can be downloaded at: https://www.mdpi.com/article/10.3390/electronics15030610/s1, Video S1: Trailer_without_stability_control_35 m/s; Video S2: Trailer_with_stability_control_35 m/s.

Funding: This research received no external funding.

Data Availability Statement: Data are contained within the article.

Conflicts of Interest: The author declares that the research was conducted in the absence of any commercial or financial relationships that could be construed as a potential conflict of interest.

Abbreviations

The following abbreviations are used in this manuscript:

ABS	Anti-Lock Braking Systems
ESC	Electronic Stability Control
LQR	Linear Quadratic Regulator
MPC	Model Predictive Control
RSC	Roll Stability Control
SMC	Sliding Mode Control

Appendix A

Parameter	Description	Value
M_1	Tractor mass	7449 kg
k_1	Radius of gyration	1.89 m
M_2	Semi-trailer mass	32,551 kg
k_2	Radius of gyration	4.05 m
a_1	Dist. tractor front-c.o.g.	1.10 m
b_1	Dist. tractor rear axle-c.o.g.	2.49 m
b_2	Dist. semitrailer axle-c.o.g.	3.15 m
a_2	Dist. kingpin semitrailer-c.o.g.	4.98 m
c_1	Dist. kingpin tractor dist.-c.o.g.	1.81 m
f	Normalized cornering stiffness	5.73 1/rad
P_d	Power (drive)	500 kW
P_b	Power (brake)	700 kW
δ_{max}	Max. steering angle	10°
$\dot{\delta}_{max}$	Max. steering rate	0.17 rad/s

References

1. Hac, A.; Fulk, D.; Chen, H. Stability and Control Considerations of Vehicle-Trailer Combination. *SAE Int. J. Passeng. Cars Mech. Syst.* **2008**, *1*, 925–937. [CrossRef]
2. Emheisen, M.A.; Emirler, M.T.; Ozkan, B. Lateral Stability Control of Articulated Heavy Vehicles Based on Active Steering System. *Int. J. Mech. Eng. Robot. Res.* **2022**, *11*, 575–582. [CrossRef]
3. Troger, H.; Zeman, K. A Nonlinear Analysis of the Generic Types of Loss of Stability of the Steady State Motion of a Tractor-Semitrailer∗. *Veh. Syst. Dyn.* **1984**, *13*, 161–172. [CrossRef]
4. Ellis, J.R. *Vehicle Handling Dynamics*; Professional Engineering Publishing: London, UK, 1994.
5. Van De Molengraft-Luijten, M.F.J.; Besselink, I.J.M.; Verschuren, R.M.A.F.; Nijmeijer, H. Analysis of the lateral dynamic behaviour of articulated commercial vehicles. *Veh. Syst. Dyn.* **2012**, *50*, 169–189. [CrossRef]
6. Anderson, J.; Kalra, N.; Stanley, K.; Sorensen, P.; Samaras, C.; Oluwatola, O. *Autonomous Vehicle Technology: A Guide for Policymakers*; RAND Corporation: Santa Monica, CA, USA, 2016. [CrossRef]

7. Litman, T. *Autonomous Vehicle Implementation Predictions'*; Victoria Transport Policy Institute: Victoria, BC, Canada, 2025. Available online: https://www.vtpi.org/avip.pdf (accessed on 17 December 2025).
8. Qin, S.J.; Badgwell, T.A. A survey of industrial model predictive control technology. *Control Eng. Pract.* **2003**, *11*, 733–764. [CrossRef]
9. Mantovani, G.; Ferrarini, L. Temperature Control of a Commercial Building with Model Predictive Control Techniques. *IEEE Trans. Ind. Electron.* **2015**, *62*, 2651–2660. [CrossRef]
10. Wang, J.-Q.; Li, S.E.; Zheng, Y.; Lu, X.-Y. Longitudinal collision mitigation via coordinated braking of multiple vehicles using model predictive control. *Integr. Comput. Aided Eng.* **2015**, *22*, 171–185. [CrossRef]
11. Di Cairano, S.; Tseng, H.E.; Bernardini, D.; Bemporad, A. Vehicle Yaw Stability Control by Coordinated Active Front Steering and Differential Braking in the Tire Sideslip Angles Domain. *IEEE Trans. Contr. Syst. Technol.* **2013**, *21*, 1236–1248. [CrossRef]
12. Zhu, B.; Tazvinga, H.; Xia, X. Switched Model Predictive Control for Energy Dispatching of a Photovoltaic-Diesel-Battery Hybrid Power System. *IEEE Trans. Contr. Syst. Technol.* **2015**, *23*, 1229–1236. [CrossRef]
13. Hrovat, D.; Di Cairano, S.; Tseng, H.E.; Kolmanovsky, I.V. The development of Model Predictive Control in automotive industry: A survey. In Proceedings of the 2012 IEEE International Conference on Control Applications, Dubrovnik, Croatia, 3–5 October 2012; pp. 295–302. [CrossRef]
14. Abroshan, M.; Hajiloo, R.; Hashemi, E.; Khajepour, A. Model predictive-based tractor-trailer stabilisation using differential braking with experimental verification. *Veh. Syst. Dyn.* **2021**, *59*, 1190–1213. [CrossRef]
15. Wang, W.; Li, G.; Liu, S. Research on Trajectory Tracking Control of a Semi-Trailer Train Based on Differential Braking. *World Electr. Veh. J.* **2024**, *15*, 30. [CrossRef]
16. Yu, H.; Li, E.; Corno, M.; Savaresi, S.M. Bi-level path tracking control of tractor semi-trailers by coordinated active front steering and differential braking. *Proc. Inst. Mech. Eng. Part D J. Automob. Eng.* **2025**, *239*, 3667–3681. [CrossRef]
17. Parra, A.; Tavernini, D.; Gruber, P.; Sorniotti, A.; Zubizarreta, A.; Pérez, J. On pre-emptive vehicle stability control. *Veh. Syst. Dyn.* **2022**, *60*, 2098–2123. [CrossRef]
18. Zhang, Y.; Khajepour, A.; Hashemi, E.; Qin, Y.; Huang, Y. Reconfigurable Model Predictive Control for Articulated Vehicle Stability with Experimental Validation. *IEEE Trans. Transp. Electrific.* **2020**, *6*, 308–317. [CrossRef]
19. Bai, Z.; Lu, Y.; Li, Y. Method of Improving Lateral Stability by Using Additional Yaw Moment of Semi-Trailer. *Energies* **2020**, *13*, 6317. [CrossRef]
20. Zhou, Q.; Zhang, H.; He, Y.; Su, Y.; Jiang, Y.; Zheng, S. A directional-performance control design for articulated heavy vehicles with extendable-trailers. *Veh. Syst. Dyn.* **2025**, *63*, 2393–2438. [CrossRef]
21. Li, G.; Fu, T.; Zhao, R. Research on Yaw Stability Control Method of Liquid Tank Semi-Trailer on Low-Adhesion Road under Turning Condition. *Appl. Sci.* **2022**, *13*, 39. [CrossRef]
22. Zhang, N.; Zhang, Q.; Zhao, Z.; Yin, G.; Li, S.; Lu, H.; Wang, C. A Phase Portrait-Based Sliding Mode Control Method to Improve Dynamic Stability of Car-Trailer Combinations via Differential Braking. *IEEE Trans. Intell. Transport. Syst.* **2025**, *26*, 19457–19467. [CrossRef]
23. Zong, C.; Zhu, T.; Wang, C.; Liu, H. Multi-objective stability control algorithm of heavy tractor semi-trailer based on differential braking. *Chin. J. Mech. Eng.* **2012**, *25*, 88–97. [CrossRef]
24. Zhao, Y.; Chen, S.; Shim, T. Investigation of Trailer Yaw Motion Control Using Active Front Steer and Differential Brake. *SAE Int. J. Mater. Manuf.* **2011**, *4*, 1057–1067. [CrossRef]
25. Tianjun, Z.; Changfu, Z. Modelling and Active Safe Control of Heavy Tractor Semi-Trailer. In Proceedings of the 2009 Second International Conference on Intelligent Computation Technology and Automation, Changsha, China, 10–11 October 2009; pp. 112–115. [CrossRef]
26. Sun, T.; He, Y.; Ren, J. Dynamics Analysis of Car-Trailer Systems with Active Trailer Differential Braking Strategies. *SAE Int. J. Passeng. Cars Mech. Syst.* **2014**, *7*, 73–85. [CrossRef]
27. Chen, L.-K.; Shieh, Y.-A. Jackknife Prevention for Articulated Vehicles Using Model Reference Adaptive Control. *Proc. Inst. Mech. Eng. Part D J. Automob. Eng.* **2011**, *225*, 28–42. [CrossRef]
28. Tian, Y.; Ma, H.; Zhang, Y.; Wen, G.; Wang, X.; Li, L. Synergistic Control Strategy for Enhanced Anti-Jackknifing Stability in Distributed-Drive Articulated Trucks. *IEEE Trans. Transp. Electrific.* **2025**, *11*, 12289–12299. [CrossRef]
29. Sun, T.; Lee, E.; He, Y. Non-Linear Bifurcation Stability Analysis for Articulated Vehicles with Active Trailer Differential Braking Systems. *SAE Int. J. Mater. Manf.* **2016**, *9*, 688–698. [CrossRef]
30. Erdinc, U.; Jonasson, M.; Kati, M.S.; Laine, L.; Jacobson, B.; Fredriksson, J. Yaw Stability Control of Vehicles Using a Slip Polytope Validated with Real Tests. In *16th International Symposium on Advanced Vehicle Control*; Mastinu, G., Braghin, F., Cheli, F., Corno, M., Savaresi, S.M., Eds.; Lecture Notes in Mechanical Engineering; Springer Nature: Cham, Switzerland, 2024; pp. 130–136. [CrossRef]
31. Kienhöfer, F.W.; Cebon, D. An investigation of ABS strategies for articulated vehicles. In Proceedings of the 8th International Symposium on Heavy Vehicle Weights and Dimensions, Johannesburg, South Africa, 14–18 March 2004; Loads, Roads and the Information Highway.

32. Skotnikov, G.I.; Jileykin, M.M.; Komissarov, A.I. Increasing the stability of the articulated lorry at braking by locking the fifth wheel coupling. *IOP Conf. Ser. Mater. Sci. Eng.* **2018**, *315*, 012027. [CrossRef]
33. Zhu, S.; He, Y. A Coordinated Control Scheme for Active Safety Systems of Multi-trailer Articulated Heavy Vehicles. In *Advances in Dynamics of Vehicles on Roads and Tracks III*; Huang, W., Ahmadian, M., Eds.; Lecture Notes in Mechanical Engineering; Springer Nature: Cham, Switzerland, 2024; pp. 824–834. [CrossRef]
34. Gao, Z.; Li, D.; Xie, L. Study on the Differential Braking of an Eddy Current Retarder Axle Used for Articulated Vehicles. In Proceedings of the 2020 IEEE 5th International Conference on Intelligent Transportation Engineering (ICITE), Beijing, China, 11–13 September 2020; pp. 596–600. [CrossRef]
35. Dunn, A.L.; Heydinger, G.J.; Rizzoni, G.; Guenther, D.A. Derivation and Validation of New Analytical Planar Models for Simulating Multi-Axle Articulated Vehicles. In Proceedings of the SAE 2004 World Congress & Exhibition, Detroit, MI, USA, 8–11 March 2004; pp. 999–1025. [CrossRef]
36. Seluga, K.J.; Obert, R.M.; Ojalvo, I.U. Articulated Vehicle Yaw Stability During Braking—A Parametric Study. In Proceedings of the SAE Commercial Vehicle Engineering Congress & Exhibition, Rosemont, IL, USA, 26–28 October 2004; pp. 248–255. [CrossRef]
37. Vempaty, S.; He, Y. A Review of Car-Trailer Lateral Stability Control Approaches. In Proceedings of the WCX^{TM} 17: SAE World Congress Experience, Detroit, MI, USA, 4–6 April 2017. [CrossRef]
38. Xin, T.; Xu, J.; Gao, C.; Sun, Z. Research on the speed thresholds of trucks in a sharp turn based on dynamic rollover risk levels. *PLoS ONE* **2021**, *16*, e0256301. [CrossRef]
39. Ikhsan, N.; Saifizul, A.A.; Ramli, R. Rollover Investigation of Two-Axle Heavy Vehicle Based on Load Transfer Ratio with Vehicle and Road Condition: A Simulation Approach. *Int. J. Automot. Mech. Eng.* **2023**, *20*, 10626–10634. [CrossRef]
40. Felez, J.; Romero, G.; Maroto, J.; Martinez, M.L. Simulation of Multi-body Systems Using Multi-bond Graphs. In *Bond Graph Modelling of Engineering Systems*; Borutzky, W., Ed.; Springer: New York, NY, USA, 2011; pp. 323–354. [CrossRef]
41. Pacejka, H.B. *Tire and Vehicle Dynamics*; Elsevier: Amsterdam, The Netherlands, 2006.

Disclaimer/Publisher's Note: The statements, opinions and data contained in all publications are solely those of the individual author(s) and contributor(s) and not of MDPI and/or the editor(s). MDPI and/or the editor(s) disclaim responsibility for any injury to people or property resulting from any ideas, methods, instructions or products referred to in the content.